Equilibrium Distributions of Dipalmitoyl Phosphatidylcholine and Dilauroyl Phosphatidylcholine in a Mixed Lipid Bilayer: Atomistic Semigrand Canonical Ensemble Simulations

Jason de Joannis, Yong Jiang, Fuchang Yin, and James T. Kindt*

Department of Chemistry and Emerson Center for Scientific Computation, Emory University, 1515 Dickey Drive, Atlanta, Georgia, 30322

Received: September 4, 2006; In Final Form: October 6, 2006

Conventional molecular dynamics (MD) simulations are seriously limited by the slow rate of diffusive mixing in their ability to predict lateral distributions of different lipid types within mixed-lipid bilayers using atomistic models. A method to overcome this limitation, using configuration-bias Monte Carlo (MC) "mutation" moves to transform lipids from one type to another in dynamic equilibrium, is demonstrated in binary fluid-phase mixtures of lipids whose tails differ in length by four carbons. The hybrid MC−MD method operates within a semigrand canonical ensemble, so that an equilibrium composition of the mixture is determined by a constant difference in chemical potential ($\Delta\mu$) chosen for the components. Within several nanoseconds, bilayer structures initiated as pure dipalmitoyl phosphatidylcholine (DPPC) or pure dilauroyl phosphatidylcholine (DLPC) converge to a common composition and structure in independent simulations conducted at the same $\Delta\mu$. Trends in bilayer thickness, area per lipid, density distributions across the bilayer, and order parameters have been investigated at three mixture compositions and compared with results from the pure bilayers at 323 K. The mixtures showed a moderate increase in DPPC acyl tail sites crossing the bilayer midplane relative to pure DPPC. Correlations between lateral positions of the two lipid types within or across the bilayer were found to be weak or absent. While the lateral distribution is consistent with nearly ideal mixing, the dependence of composition on $\Delta\mu$ indicates a positive excess free energy of mixing.

Introduction

The lateral arrangement of lipids of different molecular structure within multicomponent bilayers is an important and challenging topic in biophysical chemistry. Living organisms maintain a diverse collection of lipids with every cell and organelle membrane (and even the inner and outer leaflets of a given membrane) actively maintaining a characteristic lipid mixture, further subdivided laterally into domains.[1] While the greater part of recent discussion (and controversy) on the lateral organization of biomembranes has focused on "rafts" enriched in certain lipid, sterol, and protein types,[2−6] investigations over three decades have probed segregation, clustering, and other forms of nonideality in simple model mixed lipid bilayers.

One of the simplest types of mixed bilayer consists of lipids with identical head-groups differing only in the lengths of their hydrophobic tails. Structural and thermodynamic properties of such mixtures have been the aim of numerous experimental studies,[7−13] and tail length has been demonstrated to affect the sorting of lipids among different membranes within a living cell.[14] Mixing and demixing effects are most apparent when coupled to a phase transition, as in the temperature range between the main gel−liquid crystal transition temperatures of the two pure components; structure, thermodynamics, and growth dynamics of the gel and fluid domains in binary lipid mixtures have been investigated through a variety of simple model approaches.[15−18] Within the disordered fluid phase, nonideal mixing effects in bidisperse bilayers resist easy experimental characterization. Positive excess free energies of mixing within the fluid phase inferred from phase separation data have generally been interpreted as evidence for preferential lateral pairing of similar lipids,[8,9] but the two-dimensional (2D) lattice models on which these conclusions are based may not adequately represent interactions in the bilayer. More direct structural information is available from the "nearest neighbor recognition" (NNR) method developed by Regen et al.[19] For lipids with thiol-derivatized headgroups that cross-link reversibly, the equilibrium distribution of cross-links between like and unlike lipid types can be determined as an indicator of local mixing statistics in the bilayer. In these studies, up to 39% enhancement above random in the pairing probability of like lipids was observed in a binary fluid-phase mixture of lipids differing by 4 methylenes in their tail lengths. A similar approach has recently supplied indirect evidence for "transbilayer complementarity", or anti-correlation in the positions of long- and short-tail lipids in fluid-phase mixtures of lipids differing by only 2 methylenes per tail.[20,21] As these experiments require chemical alteration and crosslinking of lipids, it is desirable to seek support from computer simulation and other approaches to test how these observations apply to more common lipids.

Computer simulations have played an important role in the elucidation of the structure and dynamics of lipid bilayers[22,23] and membrane proteins.[24] Simulations of lipid mixtures[25−30] have been ill-equipped to address equilibrium lateral organization for a simple reason: lipid lateral diffusion is too slow. With diffusion constants of the order 10^{-8} cm^2/s, an estimated 170 ns is required for every lipid in a system to "hop" to a neighboring position;[31] simulations of at least ten times that long would be required to ensure that the final lateral distribution is

Corresponding author. E-mail: jkindt@emory.edu.

10.1021/jp065734y CCC: $33.50
Published on Web 11/23/2006

not influenced by the initial placements of different lipid types. In the most sophisticated atomistic simulation study to date of a bilayer mixture, de Vries et al.[30] performed multiple runs showing spontaneous assembly into a bilayer from disordered, homogeneous mixtures of dioleyl phosphatidylethanolamine (DOPE) and dioleyl phosphatidylcholine (DOPC) and water over a range of compositions. As the assembly is not carried out under reversible conditions, however, the resulting bilayer cannot be assumed to be equilibrated, and the results are necessarily suggestive rather than definitive. With computationally inexpensive coarse-grain (CG) models, equilibration of lateral distribution of lipid mixtures in a molecular dynamics simulation becomes tractable.[32−34] While CG models are useful, models that incorporate atomistic detail are desirable to capture the specificity of biomolecular interactions.

To circumvent barriers that slow lateral diffusion, "mutation" Monte Carlo (MC) moves have been implemented within an atomistic molecular dynamics simulation, allowing the composition at any position within the bilayer to change without the need for lipids to move across the bilayer. While the molecule targeted in each mutation attempt is chosen at random, the success probability for each attempt is determined by the local environment; mutations in positions that tend to lower the system's free energy will be preferred, leading to an equilibrium statistical sampling of arrangements of the two lipid types. Though true mixing dynamics cannot be directly addressed by this approach, the sampling of distributions can be potentially much more efficient than what is possible through diffusive mixing.

While to our knowledge this is the first report of mutation methods used to sample lipid bilayer mixtures using atomistic potentials, it builds upon well-established methods. The feasibility and effectiveness of this type of MC approach within atomistic simulations, specifically in self-assembled monolayers[35] and bulk liquid alkane mixtures[36,37] that are structurally similar to the bilayer interior, have been demonstrated by Siepmann and co-workers. MC[38] and mixed MD−MC methods[39] have previously been applied to improve the efficiency of sampling in atomistic lipid bilayer simulations. The hybrid MD−MC method developed by Chiu et al.,[39] which uses alternating blocks of MD and configuration bias[40] MC moves, has been applied to a range of bilayers and mixtures.[41,42] The use of alternating blocks might be less successful for mutation moves involving changes to chain length, where the continual gradual accommodation of the environment and the system box dimensions is necessary to allow for any significant change in composition.

In this paper, we present details of the method and its application to the dipalmitoyl phosphatidylcholine−dilauroyl phosphatidylcholine (DPPC−DLPC) mixed bilayer over a range of compositions. These components consist of two saturated acyl tails, of 16- and 12-carbons respectively, attached to identical glycero-phosphatidylcholine head-groups and are both in the fluid phase at the simulation temperature of 323 K.

Methods

In the present work, a subroutine added to the Gromacs 3.2.1[43,44] MD simulation package is used to allow for "mutation" transitions between lipids with different length tail-groups in an atomistic simulation. Mutations were performed over the course of an MD trajectory within the isomolar semigrand canonical ensemble[45] defined by constant total number of lipids, fixed difference in chemical potential $\Delta\mu$, temperature, pressure, and surface tension. Siepmann and co-workers have established configuration bias Monte Carlo[40] (CBMC) as a practical method to add and remove chains and chain fragments in atomistic simulations of alkane mixtures similar in density to the bilayer interior. The incorporation of MC moves within a hybrid MD−MC framework has been shown to be thermodynamically consistent.[46]

In the present method, each simulation step comprises a 2 fs MD step and an MC mutation attempt. The MD step is performed under conditions of constant temperature (323 K) using the stochastic (Langevin) dynamics method[47] with a thermostat time constant of 0.2 ps. This method was chosen because it is a thermostat that provides a rigorous constant temperature ensemble while operating locally; any method in which the velocities of all particles are adjusted based on the total kinetic energy of all particles is complicated to implement for a system with a variable number of particles. The force-fields for lipids were taken from Berger et al.[48] and used with the simple point charge (SPC) water model.[49] The Berendsen barostat[43] was used for semi-isotropic pressure scaling (at 1 bar pressure, zero surface tension, time constant of 1.0 ps at assumed compressibility 4.5×10^{-5} bar^{-1}) and the particle-mesh Ewald method for electrostatic forces calculated during the MD step.[50] The use of an united-atom model with charge-neutral sites for the hydrophobic tails simplifies and speeds the calculation of trial configuration energies. Bond distances are kept constant during MD steps through the SETTLE[51] and LINCS[52] algorithms.

For each mutation attempt, one lipid molecule is selected at random. Each lipid molecule is either a DLPC (di-C_{12}) or a DPPC (di-C_{16}). If a DLPC (di-C_{12}) is chosen, then new extensions to its tails are chosen through the stepwise CBMC chain growth method, with $k = 4$ positions tested at each site. Each test position, located on the surface of the sphere centered at the preceding site with radius equal to the bond radius, is drawn from a distribution weighted by the $\exp(-\beta U_{\text{bonded}})$. Here β represents $(k_B T)^{-1}$ and U_{bonded} is the sum of bending and torsional potentials associated with the new position. The selection of one of the $k = 4$ test positions is made using the nonbonded Boltzmann weight $w_{n,i} = \exp(-\beta U_{\text{non-bonded}})$, where $U_{\text{non-bonded}}$ is the Lennard-Jones potential of each test position i. (In the present model, there are no partial charges on any sites involved in mutations.) This procedure is repeated until $n = 4$ new sites are generated. The new configuration is accepted with probability $\min[1, W\,\alpha^{-1} \exp(-\beta\Delta U_{\text{end}})]$, where W is the Rosenbluth weight associated with the chain addition

$$W = \prod_{n=1}^{n_{\text{chop}}} k^{-1} \sum_{i=1}^{k} \exp[-\beta U_{\text{non-bonded}}(\mathbf{r}_{n,i})] \qquad (1)$$

ΔU_{end} is the potential energy change from changing the C_{12} sites from methyl to methylene groups, and α is the activity ratio $a_{\text{DLPC}}/a_{\text{DPPC}} = \exp(\beta\mu_{\text{DLPC}} - \beta\mu_{\text{DPPC}})$ of DLPC to DPPC in the ideal reference system. After successful DLPC → DPPC moves, the tail sites are updated with the newly generated positions and potentials (corresponding to CH_2 or CH_3 sites as appropriate), and new random velocities are selected for these sites from a Maxwell−Boltzmann distribution.

When a DPPC lipid is chosen, the acceptance probability for "chopping" the tails is given by $\min[1, W^{-1}\,\alpha \exp(+\beta\Delta U_{\text{end}})]$, which must be computed through a similar procedure in which only $k - 1$ test positions are generated at each site from the weighted distribution, and the existing site is substituted for the kth test position. Successful DPPC → DLPC moves leave unchanged the positions and velocities of all sites above the

tail cutoff. For reasons of computational convenience in interfacing with the existing Gromacs molecular dynamics code, successful chop moves do not change the intramolecular potential but only turn off the nonbonded interactions of the last four united atom (methylene and methyl) groups of each tail and switch the type of the new terminal site from CH_2 to CH_3 for purposes of calculating Lennard-Jones interactions. Therefore, "ghost" fragments trail from the ends of every DLPC tail. In principle, these fragments will have no influence on the configurational distribution of the molecules to which they are attached. The contribution to the total system energy from each fragment will be composed of bending, torsional, and kinetic energy terms. Any conformation of the molecule to which it is attached (the "real" molecule) will produce the same distribution of these energies: changes to the real molecular conformation merely shift the translational and orientational reference frame of the ghost fragment, leaving the distribution unaffected. The partition function associated with the full molecule will therefore exactly equal the product of the real interacting molecular partition function and the partition function of the ghost fragment. As the latter term depends only on intramolecular interactions and temperature, the net result is a constant shift in chemical potential that does not depend on molecular interactions. In the Results, we confirm that the presence or absence of ghost fragments in a pure DLPC bilayer has at most a small effect on bilayer dimensions and a negligible effect on C−H order parameters. While the ghost fragments have in principle no effect on the structure or the thermodynamics of mixing of DLPC, they will influence the dynamics, as DLPC tails will feel effectively higher friction and greater mass than true model DLPC. As the mutations disrupt the true dynamics of the system anyhow, this is not a serious problem.

Testing MC methods to check that the desired ensemble is being sampled is not straightforward. In the present case, we ran numerous simulations in which various parameters were changed, including the frequency of MC attempts, temperature and pressure coupling constants, and the number of trial positions k, and found that the equilibrium composition for a given value of α was unchanged within expected fluctuations. In the present system, the hybrid MC/MD simulation costs 40−50% more central processing unit (CPU) time than a conventional MD run with equal number of steps. Neighbor lists are not being used (i.e., are recalculated at every step) at present for either MD or MC. In the future, neighbor lists could be used for significant performance improvement for both MD and MC, so long as lists are recalculated after each successful mutation.

All systems contain 128 lipids and 3655 waters. Analyses of the results were performed with a combination of Gromacs utilities and python scripts. VMD[53] was used for visualization and graphics.

Results

To demonstrate the efficiency and consistency of the current method, it was applied to equilibrated 128-lipid bilayers of pure DPPC and pure DLPC in independent simulations at a common activity ratio, α. As shown in Figure 1, within 2 ns, both the compositions and the box dimensions have converged from completely different starting conditions.

Once a stable composition has been reached, mixing continues on the nanosecond time scale, as seen in Figure 2. When the MC moves are implemented, the arrangement of long and short lipids evolves significantly even over 0.1 ns, and is completely changed by 1.0 ns. The success rate for mutation moves varied between 0.001 and 0.002 at different compositions, giving an average of one mutation per 1 or 2 picoseconds; each lipid changes identity an average of 4 to 8 times per nanosecond. In contrast, when mixing occurs only through conventional molecular dynamics, the original pattern persists nearly unchanged on the nanosecond time scale.

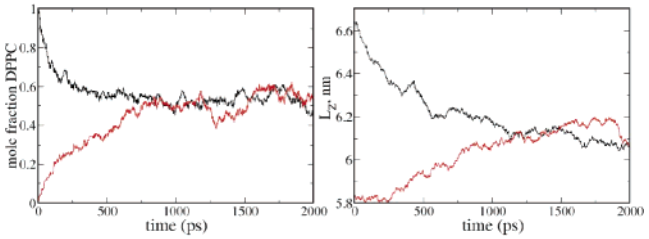

Figure 1. Rate of equilibration of system composition (left panel) and box dimension normal to bilayer L_Z (right panel) during semigrand canonical simulations initiated with pure DPPC (black curve) or pure DLPC (red curve).

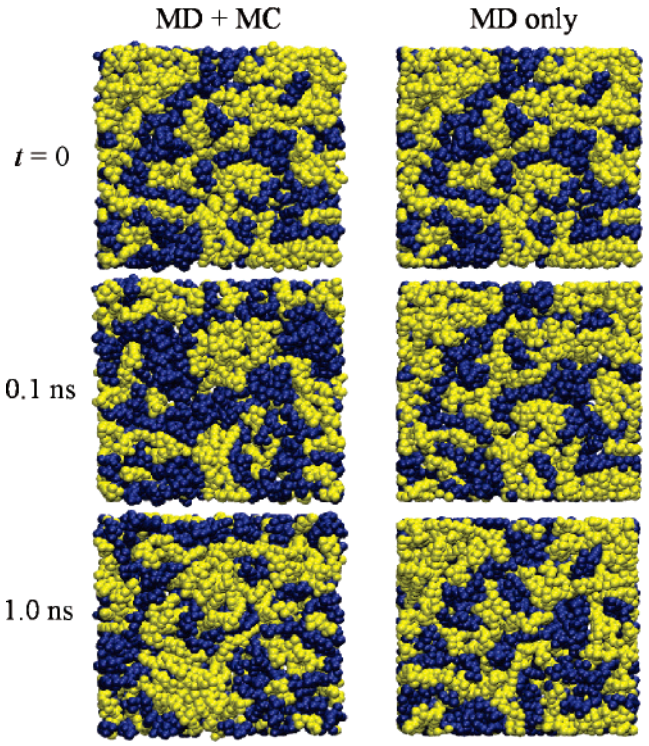

Figure 2. Top view simulation snapshots of the mixed bilayer showing evolution of distribution of DPPC (dark blue) and DLPC (yellow) over time under the hybrid method (left column) and conventional MD (right column). Solvent is omitted.

To obtain data on the structural properties of mixed bilayers, pure DPPC, pure DLPC, and three mixtures at different values of the activity ratio α were subject to equilibration for 10 ns followed by a production run of equal length. General information about the systems is shown in Table 1, while snapshots of simulated mixture cross-sections are shown in Figure 3. The excess volume of mixing of the two lipids was negligible (less than 2 $Å^3$ per molecule, or roughly 0.2% of the molecular volume), indicating that the tails of the two components pack as tightly, on average, in the mixture as in the pure bilayer. The average area per lipid of pure DPPC, determined through the semi-isotropic scaling of the box dimensions in response to the instantaneous pressure tensor, at 64.9 $Å^2$ exceeds the experimentally determined value[54] at the same temperature by 0.7 Å.[2] Consistent with a recent experimental comparison of DLPC and dimyristoyl phosphatidylcholine (DMPC),[55] we find

TABLE 1: System Composition and Dimensions[a]

activity ratio, α	mean mole fraction DLPC	mean total volume, nm^3,	ΔV_{mix}, Å^3/ lipid	mean area per lipid (Å^2),	mean system potential energy U, kJ/mol	ΔU_{mix}, per lipid, kJ/mol
0	0	272.19 ± 0.06	N/A	64.93 ± 0.31	−290206	N/A
1163	0.225 ± 0.010	265.97 ± 0.27	0.6 ± 1.7	66.68 ± 0.18	−289077	−0.19
3490	0.487 ± 0.006	258.61 ± 0.18	0.5 ± 0.9	67.10 ± 0.11	−287623	0.68
9307	0.750 ± 0.006	251.02 ± 0.19	−1.2 ± 1.1	67.01 ± 0.34	−286394	0.24
∞	1.0	244.16 ± 0.05[b] 244.15 ± 0.05	N/A	66.60 ± 0.15[b] 66.01 ± 0.13	−285082[b] −289342	N/A

[a] Uncertainties are standard errors estimated using the block-averaging method. [b] Simulation run with ghost tails.

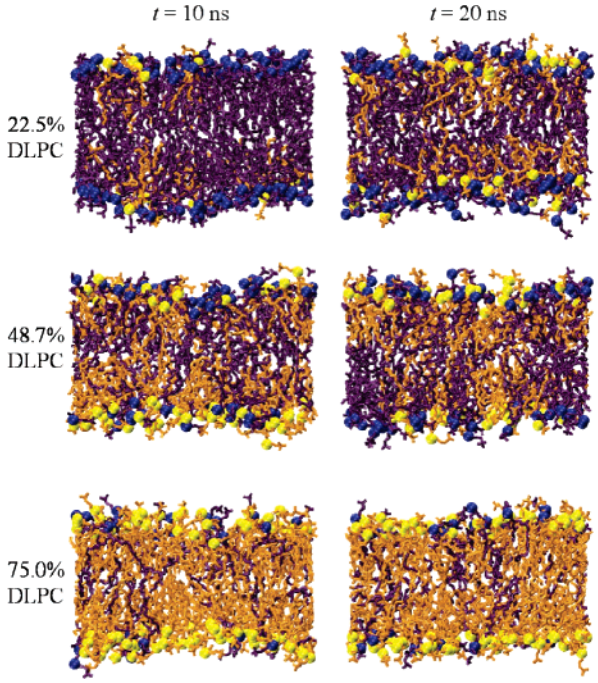

Figure 3. Snapshots of lipid bilayer cross-sections at start and end of production run. DPPC and DLPC are in purple and orange with headgroup phosphorus sites represented as blue and yellow spheres respectively. Solvent is omitted.

that the pure shorter-tailed lipid has a higher area per lipid. The average area per lipid of pure DLPC with ghost tails, which according to the arguments presented in Methods should be the same as the value without ghosts, was higher by 0.6 Å.[2] Whether this difference reflects a small bias introduced by the presence of the ghost tails or just statistical fluctuations is not yet certain; the standard deviations (±0.7 Å^2) in the two distributions overlap even though the standard errors, estimated using the block-averaging method,[56] do not. Within the three sets of mixed bilayers, area per lipid shows little dependence on composition. The mixtures showed slightly higher mean lipid areas than the pure bilayers.

Bilayer thickness, defined here as the distance between the average phosphorus site Z-coordinates of the two leaflets, is approximately linear in composition as shown in Figure 4, with a slight upward concavity. A similar deviation from linearity was evident in thickness data derived from NMR measurements of fluid phase DMPC−distearoyl phosphatidylcholine (DSPC) mixtures (ref 11, Figure 10). Within the mixed bilayers, the mean DPPC thickness was slightly above the average for the whole bilayer, while the mean DLPC thickness was slightly below the average; that is, the average DPPC phosphorus headgroup site was slightly farther from the bilayer midplane than the average DLPC phosphorus. In comparison to the root mean square deviation of this site's distribution normal to the bilayer (∼7 Å), the differences were quite small with the greatest at 0.35 Å seen at 25% DLPC. The slightly smaller mean

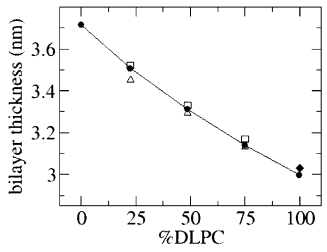

Figure 4. Bilayer thickness (calculated as distance between phosphorus site distributions) vs composition. Black circles: average thickness calculated from all lipids. Open squares: thickness calculated from DPPC alone. Open triangles: thickness calculated from DLPC alone. Black diamond indicates thickness of control simulation run without ghost tails.

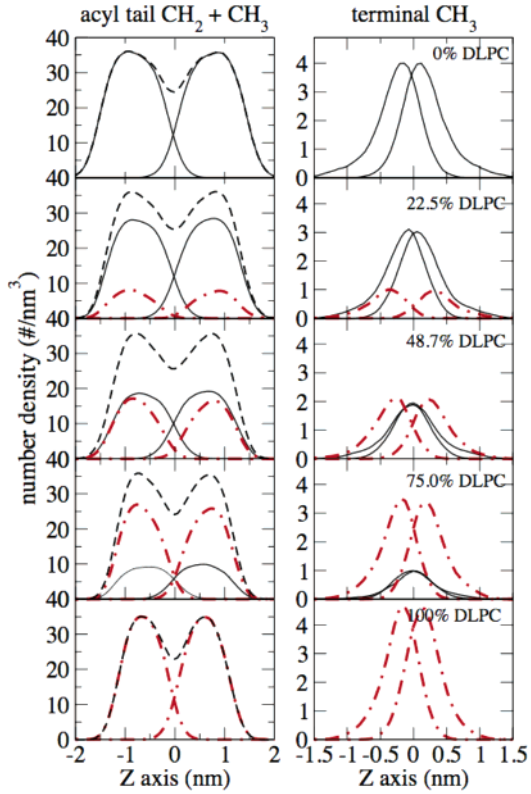

Figure 5. Total acyl chain (left) and terminal methyl (right) site density distributions normal to the bilayer. Solid curves: DPPC. Dotted and dashed red curves: DLPC. Dashed curves: total.

thickness seen in pure DLPC with ghost tails represents about a 1% decrease, as expected from the 1% increase in area per lipid.

The total density profiles of lipid acyl tail sites normal to the bilayer are shown according to lipid type and leaflet origin in Figure 5 (left column). The total density distribution of tail sites varies in a smooth manner from pure DPPC to pure DLPC with no significant change in the maximum and minimum values in the site density distributions. The longer DPPC tails contribute most of the density within 0.5 nm of the bilayer mid-plane.

TABLE 2: Integrated Site Density Across the Bilayer Midplane in Pure and Mixed Bilayers

	mean number of midplane-crossing sites per lipid		
mole fraction DLPC	Total average	DPPC	DLPC
0	1.71	1.71	N/A
0.225	1.87	2.32	0.32
0.487	2.04	3.25	0.73
0.750	1.68	3.98	0.92
1.0	1.40	N/A	1.40

Looking specifically at the methyl tail sites (Figure 5, right column), we see that the methyl group distributions of the long-tail lipids of either leaflet at 48.7 or 75% DLPC are nearly superimposable, centered at the bilayer midplane. As a measure of the overlap between leaflets, the mean number of CH_3 or CH_2 sites per lipid positioned across the bilayer midplane has been calculated and listed in Table 2. The maximum overall degree of translayer intermingling is found at 2.05 sites for the 1:1 mixture, which is only moderately higher than the value of 1.71 obtained for the pure DPPC bilayer. The great majority of sites crossing over are naturally DPPC sites.

The occupation of a central zone by DPPC tail ends from both leaflets suggests significant translayer interactions by the long-tailed lipids, which can conceivably couple the distribution of long and short lipids on one leaflet with the distribution on the opposite leaflet; it is natural to propose that DPPC will tend to face DLPC on the opposite leaflet to reduce steric hindrance between DPPC tails. This idea, invoked in the discussion of mixed-bilayer thicknesses,[11] has been pursued experimentally through NNR experiments by Regen and co-workers[20,21] and examined in simulations involving coarse-grained[57] and toy model simulations.[58] Conversely, preferential pairing of like lipids within a leaflet within the fluid phase has been inferred from indirect thermodynamic evidence[8,9] and quantified through the NNR method.[19] As no such correlations were apparent through casual inspection of snapshots, we have sought statistical evidence for these behaviors in the present simulations. Radial distribution functions showing the correlations between lipid center-of-mass positions projected on the $X-Y$ plane are shown in Figure 6. The left column gives intra-leaflet correlations, which drop as $r \rightarrow 0$ due to steric repulsion between lipids. Correlations between like and unlike lipid types show little deviation, indicating to a first approximation a random distribution of lipid types within each leaflet. The right column gives cross-leaflet correlations, which do not vanish as $r \rightarrow 0$. If lipid positions within the two leaflets were completely uncorrelated, $g(r)$ would equal one for all r. Differences at higher values of r are more significant than at low values of r. At very low r, the sampling becomes poor, as (even in an uncorrelated system) the chance of two lipids' centers of mass being found at very nearly the same lateral position is small.

To represent the same data in a way that better emphasizes its significance, in Figure 7 we plot the integrated mean excess number of like lipids as a function of r; that is, out of all the lipids whose center-of-mass lie within a lateral distance r of lipid A, the difference between the observed number of lipids of type A and the number expected if the lipid type were

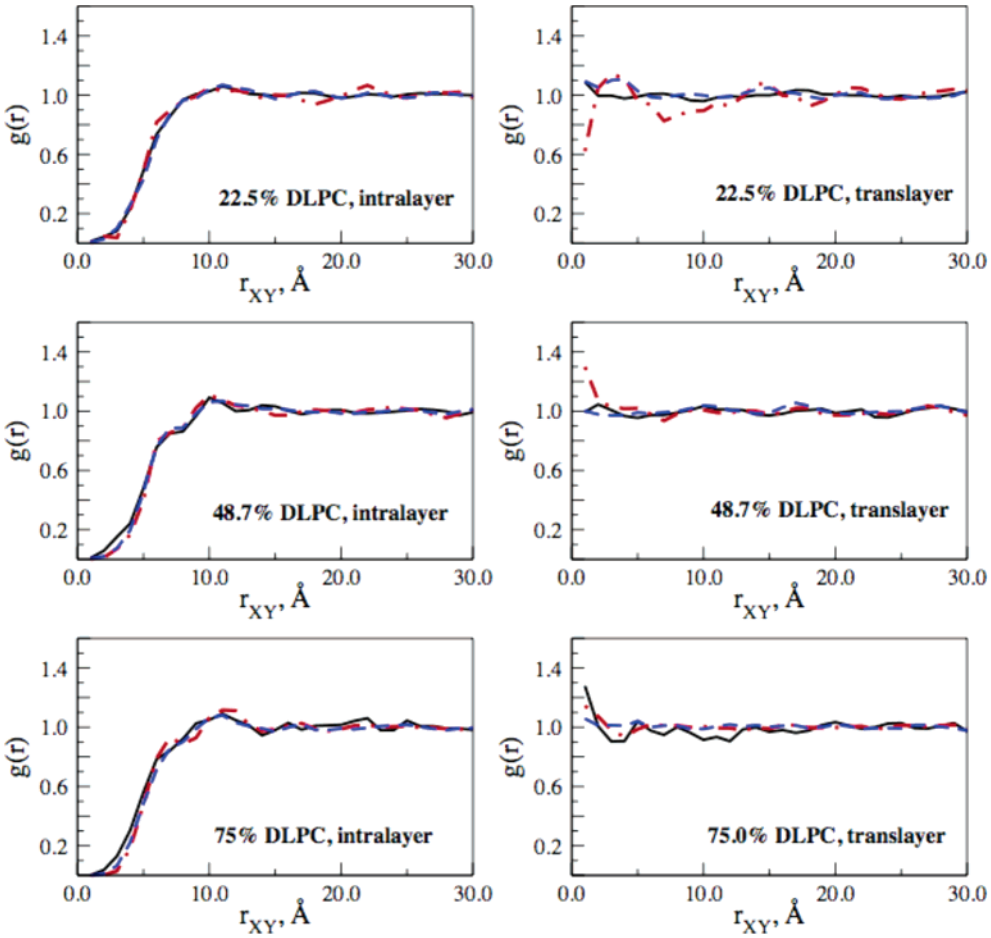

Figure 6. Lateral center-of-mass radial distribution functions for intra- (left) and inter- (right) leaflet correlations. Solid black lines: DPPC−DPPC. Dash-dot red lines: DLPC−DLPC. Dashed blue lines: DLPC−DPPC.

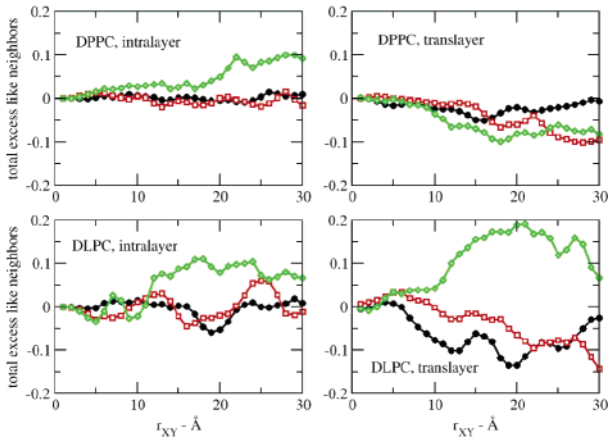

Figure 7. Mean excess number of lipids of same type with center of mass within a lateral distance r_{XY} from integration of data in Figure 6. Black circles: 22.5% DLPC. Red open squares: 48.7% DLPC. Green open diamonds: 75% DLPC.

uncorrelated to the center-of-mass position. Within the leaflets, there is no significant correlation in the 22.5 and 48.7% DLPC trajectories, and a mean excess balance of 0.1 like lipid in the neighborhood of either type of lipids at 75% DLPC. Transbilayer complementarity effects appear to be weak as well; within a radius of 10 Å, which will include on average ~5 nearest lipids on the facing leaflet, no significant defect is discernible. "Perfect" transbilayer complementarity in which every lipid is matched to a nearby lipid of complementary length on the opposite leaflet would give an excess of −0.5 in the 50:50 mixture. A defect of 0.1 molecule does appear at longer distances for the 48.7% DLPC mixture. This may reflect a delocalized effect, but as values at larger distance represent small differences between increasing numbers of neighbors, it is difficult to rule out random fluctuations.

The C−H bond order parameters of both components, averaged over both chains and all protons bound to each acyl carbon, are shown for the mixtures and compared with the pure bilayers in Figure 8. For the 1:3 and 1:1 DLPC/DPPC mixtures, the ordering of carbons 2−5 (the "plateau region") is very similar for the two lipids within the mixture, while methylene groups 6−11 belonging to DPPC are moderately more ordered than corresponding groups in DLPC. The general degree of tail ordering in the mixture is intermediate between the two pure bilayers; the presence of DPPC has a straightening effect on DLPC, while the presence of DLPC has a disordering effect on DPPC. The behavior in these two cases is in good qualitative agreement with experimental data on fluid DMPC−DSPC mixtures,[13] although the present results indicate a greater overall disordering effect. For instance, where experimentally a 1:1 mixture showed changes of roughly equal magnitude (opposite in sign) for the two components relative to the pure systems, in the present simulation the decrease in DPPC order exceeds the increase in DLPC order. The 75% DLPC mixture shows a qualitative difference from the others: the longer-tailed DPPC lipid is actually less ordered than DLPC, most notably in the plateau region. Finally, by this measure, the influence of the ghost tails on the structure of the pure DLPC bilayer can be seen to be very minor.

Aside from its use in achieving efficient mixing, the semigrand ensemble method gives information about the thermodynamics of mixing through the relationship between activity ratio and composition. In an ideal mixture of N_A lipids of type A and N_B lipids of type B and satisfying a free energy expression

$$F(N_A,N_B) = N_A(\mu_A^0 + k_BT\ln N_A) + N_B(\mu_B^0 + k_BT\ln N_B) \quad (2)$$

with μ^0 being the chemical potential in the pure bilayer, the activity ratio will be directly proportional to the mole ratio $X \equiv N_A/N_B$ of the components

$$\alpha(X) = \exp[\beta\mu_A(N_A,N_B) - \beta\mu_B(N_A,N_B)] = X\exp(\beta\mu_A^0 - \beta\mu_B^0). \quad (3)$$

The chemical potentials μ_A and μ_B are obtained from differentiating F with respect to N_A or N_B. The activity ratios of DLPC/DPPC mixtures at 323 K, shown in Figure 9, show some deviation from the ideal linear dependence on mole ratio. Introducing a term to account for this nonideality at the second virial approximation[59]

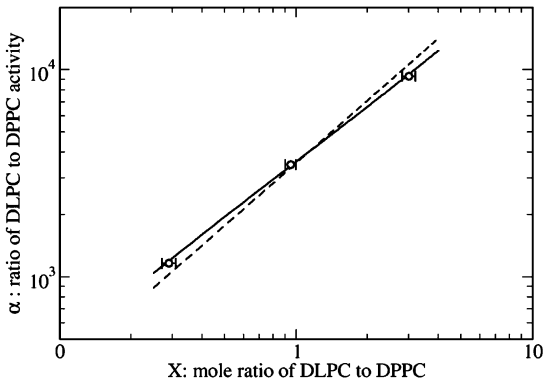

Figure 9. Activity ratio vs mole ratio from simulations (circles). Dashed line shows ideal model fit; solid curve shows nonideal fit using eq 5 with $B = 0.5$.

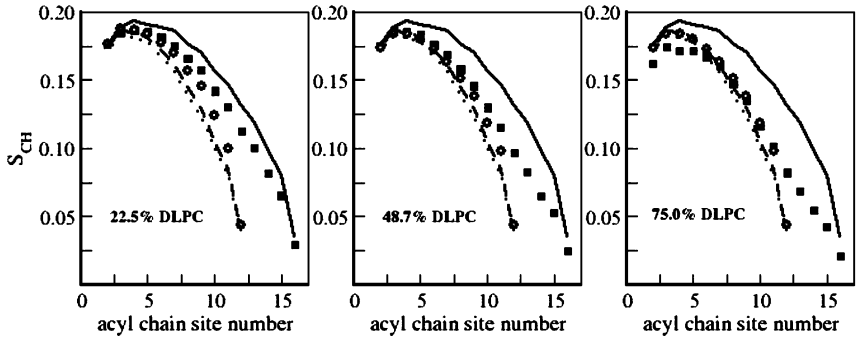

Figure 8. C−H bond order parameters for methylene and methyl groups of lipid acyl tails by position in the tail, averaged over all protons on both tails. Filled squares: DPPC in mixture. Open circles: DLPC in mixture. Solid curve: pure DPPC data. Dashed and dotted curves: DLPC with and without ghost tails.

$$F(N_A,N_B) = N_A(\mu_A^0 + k_BT\ln N_A) + N_B(\mu_B^0 + k_BT\ln N_B) + \frac{k_BT}{2}B\frac{N_AN_B}{N_A+N_B} \quad (4)$$

leads to

$$\alpha(X) = X\exp(\beta\mu_A^0 - \beta\mu_B^0)\exp\left(\frac{B(1-X)}{2+2X}\right) \quad (5)$$

With only three points, we cannot seriously test the appropriateness of eq 5 to fit the data or derive a value of the dimensionless second virial coefficient B with any real precision; reasonable fits to the data are possible with B in the range from $+0.3$ to $+0.6$, indicating a positive excess free energy of mixing. While the model of eqs 4 and 5 assumes that the nonideality is symmetric with respect to the lipid type, the data suggest slightly greater deviation from ideality at high DLPC than at low DLPC.

Discussion

Efficiency and Applicability of the Methods. The success rate of mutation MC moves in the present system, 0.001, is high enough to make the method significantly more efficient than pure MD for resolving the equilibrium statistics of mixing of DLPC and DPPC. The equilibration is not limited by the rate of mixing but by the slow collective modes, fluctuations of bilayer area and thickness with relaxation times of several nanoseconds,[60] common to all bilayer simulations. Mutation success rates will be strongly dependent on system details; for instance, we have found moves that involve mutations of six carbons on both tails have unacceptably low acceptance probabilities. Use of a multistep mutation approach[61] may enable the application of the method to mixtures with greater tail length differences. Mutations of headgroup sites in close contact with solvent are also likely to present new challenges, including the computational expense of calculating long-ranged electrostatic interaction energies for each trial MC position; the use of a united-atom forcefield without partial charges on the tail sites simplified the present study.

Structure of the Mixed Bilayer. From phosphorus site distributions and order parameters, it is apparent that the headgroups of the two lipid types are conformationally nearly indistinguishable, particularly at 22.5 and 48.7% DLPC. Taking together the observations of density profiles and order parameters, the structure of these mixtures appears to be quite consistent with the picture of DMPC/DSPC fluid mixtures described by Lu et al.[13] on the basis of NMR measurements of smoothed C−D bond order parameters. The DPPC tails extend to fill in a disordered zone around the bilayer midplane in which they have significant overlap with the opposing leaflet. However, as the DLPC have much lower overlap, the total degree of overlap or interdigitation is only moderately increased in the mixed bilayers relative to the pure DPPC. In the system where DPPC was a minority component, its first few tail carbons were significantly less ordered than those of the DLPC in the mixture or even in pure DLPC. This suggests that the longer tails are strongly perturbed by the thinness of the bilayer and adapt by tilting or kinking near the headgroup.

Correlations between lateral positions were nearly independent of lipid type; pairwise distance distribution functions showed little significant difference between like and unlike pairs. Integrated correlation functions showed at most a mean excess or deficit of 0.1 lipids of the same type in the vicinity (3 nm radius, either on the same or the opposing leaflet) of a given lipid. Preferential pairing of like lipids within the leaflet, determined through NNR experiments[19] to be as high as 39% within a fluid phase of modified lipids with the same tail length mismatch as in the present simulation, was not apparent in anywhere near the same degree in the trajectories observed. The experimental evidence for transbilayer complementarity is less easily quantified,[21] but the present simulations tend to suggest that the transbilayer interactions of the longer lipid have only a weak influence on the arrangement of the two lipid types at equilibrium in the present model system. (The present simulation data do *not* contradict the CG simulation results of Stevens[57] in which complementarity was observed in ordered gel-phase domains; in the present work, as in the experiments of refs 20 and 21, the temperature is above the gel phase transition temperatures of both components.) This result, like any result about equilibrium structures drawn from trajectory calculations, is only reliable so far as no long-time relaxation process is necessary to allow the structure to achieve its stability. The MC−MD method has successfully reduced the time scale for lipids to reversibly exchange places, but some other rearrangement necessary to stabilize a certain pattern may be rate limiting. Longer trajectories and a greater variety of starting conformations will be necessary to confirm that these results hold for the present model system. The model system is another issue both in experiment and in simulation. The NNR experiments can only be performed using modified lipids that are chemically crosslinked at the headgroup. The present simulations do not attempt to model those experiments directly but are an attempt to represent a mixture of common phospholipids. We will not presume to know whether the experimental system with its real structural differences, or the simulation model with its approximate force-field, is better suited for predicting the behavior of the real DPPC/DLPC mixture.

Thermodynamics of Mixing. While the structures did not indicate significant deviation from random lateral distributions, the relationship between composition and activity ratio showed a small but significant deviation from ideal behavior indicating a positive excess free energy of mixing. Within a 2D hexagonal lattice model, such as the one that has been used to interpret experimental evidence of nonideal mixing,[8,9] the rough magnitude of the nonideality would suggest a free energy preference of the order 0.05 k_BT to 0.1 k_BT for neighboring pairs of the same type, and a probability of 2.5−5% above random to find neighboring pairs of like type. Even such a modest enhancement would not be consistent with the weak lateral correlations observed in the radial distribution functions discussed above. The results suggest that the thermodynamic nonideality of mixing in the current system arises from collective mean-field effects (accommodation of different length lipids within a bilayer of changing thickness being the most obvious) rather than from localized interactions between neighboring pairs of lipids. More data will be needed to test the applicability of various models for these effects.

Conclusions

The present study has shown the usefulness of a hybrid MC−MD semigrand ensemble method in the simulation of a bidisperse mixed bilayer of phosphatidylcholine lipids. The strong dependence of lateral distributions on starting configuration, which is unavoidable in all but extremely long simulations, is removed at only a moderate extra computational expense. There will certainly be limitations in the types of lipid mixtures for which this approach will succeed; a greater than 4-carbon difference in tail length cannot be practically accommodated using the current algorithm, but some of these barriers

may be surmountable. We anticipate that this method can be used to give insight into the equilibrium distribution of different lipid types among the various microenvironments present in biological membranes, for instance, in the vicinity of transmembrane proteins.

The structure of the DLPC/DPPC mixed model bilayer shows similar trends in bilayer thickness and order parameter to those measured in similar fluid-phase lipid mixtures. Within the mixtures, a zone around the bilayer midplane is occupied almost exclusively by the tails of the longer component lipid from both leaflets. The total extent of this intermingling is moderately greater than in pure DPPC. Differences between the two components' headgroup positions and the position and order of the first few carbons in the acyl chains are very small except in the 75% DLPC system, which showed a significant disordering at all positions on the DPPC acyl tail. Strong local lateral correlations in composition are not observed, neither pairing within leaflets nor complementary matching across the leaflets. While lateral mixing is nearly statistical from the structural perspective, a small but significant positive excess free energy of mixing can be inferred from the dependence of composition on activity ratio. In contrast to the predictions of simple models, this nonideal mixing behavior is not reflected by local demixing.

Acknowledgment. We thank the National Science Foundation (Grant CHE-0616383), the Arthur P. Sloan Foundation, and the Camille and Henry Dreyfus Foundation for financial support. Hao Wang, Jeffrey Gaulding, and Kunal Khanna are acknowledged for their assistance in testing the simulation code, and Patrick Coppock for generating control data on pure DPPC.

References and Notes

(1) Glaser, M. *Curr. Opin. Struct. Biol.* **1993**, *3*, 475−481.
(2) Edidin, M. *Curr. Opin. Struct. Biol.* **1997**, *7*, 528−532.
(3) Rietveld, A.; Simons, K. *Biochim. Biophys. Acta.* **1998**, *1376*, 467−479.
(4) Jacobson, K.; Dietrich, C. *Trends Cell Biol.* **1999**, *9*, 87−91.
(5) Mukherjee, S.; Maxfield, F. R. *Traffic* **2000**, *1*, 203−211.
(6) Edidin, M. *Trends Cell Biol.* **2001**, *11*, 492−496.
(7) Mabrey, S.; Sturtevant, J. M. *Proc. Nat. Acad. Sci. U.S.A.* **1976**, *73*, 3862.
(8) Lee, A. G. *Biochim. Biophys. Acta.* **1977**, *472*, 285−344.
(9) Von Dreele, P. H. *Biochemistry* **1978**, *17*, 3939−3943.
(10) Knoll, W.; Ibel, K.; Sackmann, E. *Biochemistry* **1981**, *20*, 6379−6383.
(11) Sankaram, M. B.; Thompson, T. E. *Biochemistry* **1992**, *31*, 8258−8268.
(12) Garidel, P.; Blume, A. *Biochim. Biophys. Acta.* **1998**, *1371*, 83−95.
(13) Lu, D.; Vavasour, I.; Morrow, M. R. *Biophys. J.* **1995**, *68*, 574−583.
(14) Mukherjee, S.; Soe, T. T.; Maxfield, F. R. *J. Cell Biol.* **1999**, *144*, 1271−1284.
(15) Jorgenson, K.; Sperotto, M. M.; Mouritsen, O. G.; Ipsen, J. H.; Zuckermann, M. J. *Biochim. Biophys. Acta.* **1993**, *1152*, 135−145.
(16) Sugar, I. P.; Thompson, T. E.; Biltonen, R. L. *Biophys. J.* **1999**, *76*, 2099−2110.
(17) Michonova-Alexova, E. I.; Sugar, I. P. *Biophys. J.* **2002**, *83*, 1820−1833.
(18) Shi, Q.; Voth, G. A. *Biophys. J.* **2005**, *89*, 2385−2394.
(19) Dewa, T.; Miyake, Y.; Kézdy, F. J.; Regen, S. L. *Langmuir* **2000**, *16*, 3735−3739.
(20) Zhang, J.; Jin, B.; Tokutake, N.; Regen, S. L. *J. Am. Chem. Soc.* **2004**, *126*, 10856−10857.
(21) Zhang, J.; Jing, B.; Regen, S. L. *Langmuir* **2005**, *21*, 8983−8986.
(22) Scott, H. L. *Curr. Opin. Struct. Biol.* **2002**, *12*, 495−502.
(23) Tobias, D. J.; Tu, K. C.; Klein, M. L. *Curr. Op. Colloid Interf. Sci.* **1997**, *2*, 15−26.
(24) Ash, W. L.; Zlomislic, M. R.; Oloo, E. O.; Tieleman, D. P. *Biochim. Biophys. Acta.* **2004**, *1666*, 158−189.
(25) Bandyopadhyay, S.; Tarek, M.; Klein, M. L. *J. Phys. Chem. B* **1999**, *103*, 10075−10080.
(26) Schneider, M. J.; Feller, S. E. *J. Phys. Chem. B* **2001**, *105*, 1331−1337.
(27) Bandyopadhyay, S.; Shelley, J. C.; Klein, M. L. *J. Phys. Chem. B* **2001**, *105*, 5979−5986.
(28) Balali-Mood, K.; Harroun, T. A.; Bradshaw, J. P. *Eur. Phys. J. E* **2003**, *12*, s135−s140.
(29) Gurtovenko, A. A.; Patra, M.; Karttunen, M.; Vattulainen, I. *Biophys. J.* **2004**, *86*, 3461−3472.
(30) de Vries, A. H.; Mark, A. E.; Marrink, S. J. *J. Phys. Chem. B* **2004**, *108*, 2454−2463.
(31) Pastor, R. W.; Feller, S. E. In *Biological Membranes: A Molecular Perspective from Computation and Experiment*; Merz, K. M., Roux, B., Eds.; Birkhauser: Boston, MA, 1996.
(32) Faller, R.; Marrink, S.-J. *Langmuir* **2004**, *20*, 7686−7693.
(33) Nielsen, S. O.; Lopez, C. F.; Ivanov, I.; Moore, P. B.; Shelley, J. C. *Biophys. J.* **2004**, *87*, 2107−2115.
(34) de Joannis, J.; Jiang, F. Y.; Kindt, J. T. *Langmuir* **2006**, *22*, 998−1005.
(35) Siepmann, J. I.; McDonald, I. R. *Mol. Phys.* **1992**, *75*, 255−259.
(36) Martin, M. G.; Siepmann, J. I. *J. Am. Chem. Soc.* **1997**, *119*, 8921−8924.
(37) Stubbs, J. M.; Siepmann, J. I. *J. Phys. Chem. B* **2002**, *106*, 3968−3978.
(38) Jedlovszky, P.; Mezei, M. *J. Chem. Phys.* **1999**, *111*, 10770−10773.
(39) Chiu, S.-W.; Clark, M.; Jakobsson, E.; Subramaniam, S.; Scott, H. L. *J. Comp. Chem.* **1999**, *20*, 1153−1164.
(40) Siepmann, J. I.; Frenkel, D. *Mol. Phys.* **1992**, *75*, 59−70.
(41) Chiu, S.-W.; Jakobsson, E.; Scott, H. L. *J. Chem. Phys.* **2001**, *114*, 5435−5443.
(42) Chiu, S.-W.; Jakobsson, E.; Mashl, R. J.; Scott, H. L. *Biophys. J.* **2002**, *83*, 1842−1853.
(43) Berendsen, H. J. C.; van der Spoel, D.; van Drunen, R. *Comput. Phys. Comm.* **1995**, *91*, 43−56.
(44) Lindahl, E.; Hess, B.; van der Spoel, D. *J. Mol. Model* **2001**, *7*, 306−317.
(45) Kofke, D. A. In *Advances in Chemical Physics: Monte Carlo Methods in Chemical Physics*; Ferguson, D. M., Siepmann, J. I., Truhlar, D. G., Eds.; Interscience: New York, 1998; Vol. 105, p 405−441.
(46) LaBerge, L. J.; Tully, J. C. *Chem. Phys.* **2000**, *260*, 183−191.
(47) van Gunsteren, W. F.; Berendsen, H. J. C. *Mol. Simul.* **1988**, *1*, 173−185.
(48) Berger, O.; Edholm, O.; Jähnig *Biophys. J.* **1997**, *72*, 2002−2013.
(49) Berendsen, H. J. C.; Postma, J. P. M.; van Gunsteren, W. F.; Hermans, J. In *Intermolecular Forces*; Pullman, B., Ed.; D. Reidel: Dordrecht, The Netherlands, 1981.
(50) Essman, U.; Perera, L.; Berkowitz, M. L.; Darden, T.; Lee, H.; Pedersen, L. G. *J. Chem. Phys.* **1995**, *103*, 8577−8592.
(51) Miyamoto, S.; Kollman, P. A. *J. Comp. Chem.* **1992**, *13*, 952−962.
(52) Hess, B.; Bekker, H.; Berendsen, H. J. C.; Fraaije, J. G. E. M. *J. Comp. Chem.* **1997**, *18*, 1463−1472.
(53) Humphrey, W.; Dalke, A.; Schulten, K. *J. Mol. Graphics* **1996**, *14*, 33−38.
(54) Kucerka, N.; Tristram-Nagle, S.; Nagle, J. F. *Biophys. J.* **2006**, *90*, L83−L85.
(55) Kucerka, N.; Liu, Y.; Chu, N.; Petrache, H.; Tristram-Nagle, S.; Nagle, J. F. *Biophys. J.* **2005**, *88*, 2626−2637.
(56) Allen, M. P.; Tildesley, D. J. *Computer Simulation of Liquids*; Oxford University Press: Oxford, England, 1987.
(57) Stevens, M. J. *J. Am. Chem. Soc.* **2005**, *127*, 15330−15331.
(58) Khanna, K.; Chang, T. T.; Kindt, J. T. *J. Chem. Phys.* **2006**, *124*, 036102.
(59) Hill, T. L. *An Introduction to Statistical Thermodynamics*; Dover: Mineola, NY, 1986.
(60) Lindahl, E.; Edholm, O. *Biophys. J.* **2000**, *79*, 426−433.
(61) Escobedo, F. A.; de Pablo, J. J. *J. Chem. Phys.* **1996**, *105*, 4391−4394.